First in situ X-ray identification of coesite and retrograde quartz on a glass thin section of an ultrahigh-pressure metamorphic rock and their crystal structure details

Daijo Ikuta,[1,*] Naoyuki Kawame,[1] Shohei Banno,[2] Takao Hirajima,[2] Kazuhiko Ito,[3]
John F. Rakovan,[4] Robert T. Downs,[5] and Osamu Tamada[1]

[1]Graduate School of Human and Environmental Studies, Kyoto University, Sakyoku, Kyoto 606-8501, Japan
[2]Graduate School of Science, Department of Geology and Mineralogy, Kyoto University, Sakyoku, Kyoto 606-8502, Japan
[3]Faculty of Management Information, Taisei Gakuin University, Sakai, Osaka 587-8555, Japan
[4]Department of Geology, Miami University, Oxford, Ohio 45056, U.S.A.
[5]Department of Geosciences, University of Arizona, Tucson, Arizona 85721-0077, U.S.A.

ABSTRACT

To ensure the presence of coesite and its transformed polymorph, quartz, in ultrahigh-pressure (UHP) rocks and to examine the relic of the phase transformation, crystal structures were analyzed by single-crystal X-ray diffraction (XRD) directly using the rock thin section mounted on a slide glass. The rock sample used is a coesite-bearing eclogite from the Sulu UHP terrain, eastern China. The crystal structures were determined successfully by this new method and the presence of coesite and quartz in UHP rocks was identified for the first time by XRD. The R-factor $[R(F)]$ converged to 0.046 for coesite and 0.087 for quartz. The displacement ellipsoids for coesite and quartz are larger than those previously reported for these two phases, which is consistent with expected effects of trapped strain due to the phase transformation from coesite to quartz during exhumation from the Earth's mantle.

This paper is the first report of single-crystal XRD of a rock thin section on a glass slide and establishes the technique, and provides proof-of-concept of the method. Although the mineral species included in a thin section can often be identified by other methods, such as Raman spectroscopy, an advantage of the reported method is that it can be applied to any mineral in a thin section, and not just to the UHP minerals. Moreover, it is applicable to an unknown or new mineral in a thin section, discarding the spots of known minerals and constructing a lattice from the residual spots to find the structure of the unknown phase.

Keywords: Crystal structure, coesite, quartz, UHP rock, thin section, XRD, displacement ellipsoid

INTRODUCTION

In 1984, coesite was reported in crustal metamorphic rocks of the eclogite facies in two areas of Europe: pyrope-quartzite in the Dora Maira Massif of the Western Alps (Chopin 1984) and in dolomite-eclogite from the Western gneiss region of Norway (Smith 1984). In 1990, diamond inclusions were found in garnet from metamorphic rocks derived from crustal materials in the Kokchetav Massif, Kazakhstan (Sobolev and Shatsky 1990). These epoch-making discoveries initiated the study of ultrahigh-pressure (UHP) metamorphism. The rocks, which include coesite or diamond and are equilibrated at the equivalent depth of coesite or diamond stability, have now been found in more than 20 places on the planet (see Carswell and Compagnoni 2003).

Identification of coesite in UHP rocks has been accomplished through a combination of compositional analysis by electron microprobe and optical observations including: (1) the texture of polycrystalline quartz aggregate, (2) radial cracking of host minerals such as garnet and omphacite, (3) refractive index, and (4) other optical characters (e.g., Chopin 1984; Hirajima et al. 1990). Raman spectroscopy also has been regarded as a powerful tool for the identification of coesite (e.g., Tabata et al. 1998).

There are a few transmission electron microscopic studies for the deformation mechanism of quartz-coesite inclusions in UHP rocks (Ingrin and Gillet 1986; Langenhorst and Poirier 2002). These studies identified the minerals by electron diffraction. At present however, the XRD technique is a more reliable and quantitative method for determining mineral species and structure than spectroscopy or other methods. However, XRD has not been adopted for the identification or structure analysis of coesite and quartz in UHP rocks because it is hard to pick out the required tiny single crystals. It has, therefore, been required to develop a new X-ray method to analyze tiny and rare minerals (like coesite and quartz) surrounded by other phases in UHP rocks.

The XRD method for minerals in a thin section mounted on a glass slide is established in this study. This study aims to develop the technique for the direct identification of phases in a thin section, and to determine the details of their crystal structures and relative orientations, and, in particular, to apply the technique to coesite and quartz in UHP metamorphic rocks.

EXPERIMENTAL METHODS AND RESULTS

UHP rock sample and coesite

The rock sample used in this study is a fragment of a coesite eclogite collected from the Yangkou meta-igneous complex in the middle part of the Sulu UHP ter-

---

rain, eastern China (Hirajima et al. 1993; Wallis et al. 1997). The coesite eclogite is foliated, fine-grained, and mainly composed of garnet, omphacite, and phengite, with minor amounts of coesite, kyanite, rutile, and retrograde quartz. Coesite that is partly decomposed occurs not only as an included phase in the main garnet and omphacite matrix, but also as one of the main matrix phases. Peak *P-T* conditions of the eclogite at the UHP stage have been estimated as 700–800 °C and 3.1–4.1 GPa (Hirajima and Nakamura 2003). The garnet peridotite, which is also a member of the Yangkou meta-igneous complex, shows similar *P-T* conditions at the UHP stage and records the adiabatic isothermal decompression path from the mantle (ca. 90–120 km deep) to the lower crust (ca. 30–50 km deep) (Yoshida et al. 2004).

Initially, quartz and coesite were rarely found in thin sections of the sample, even under careful microscopic observation. This rarity contributed to the long-veiled existence of UHP metamorphic rocks. But now that coesite is known to be in the rocks, it is not so difficult to find, because it is usually mantled by quartz
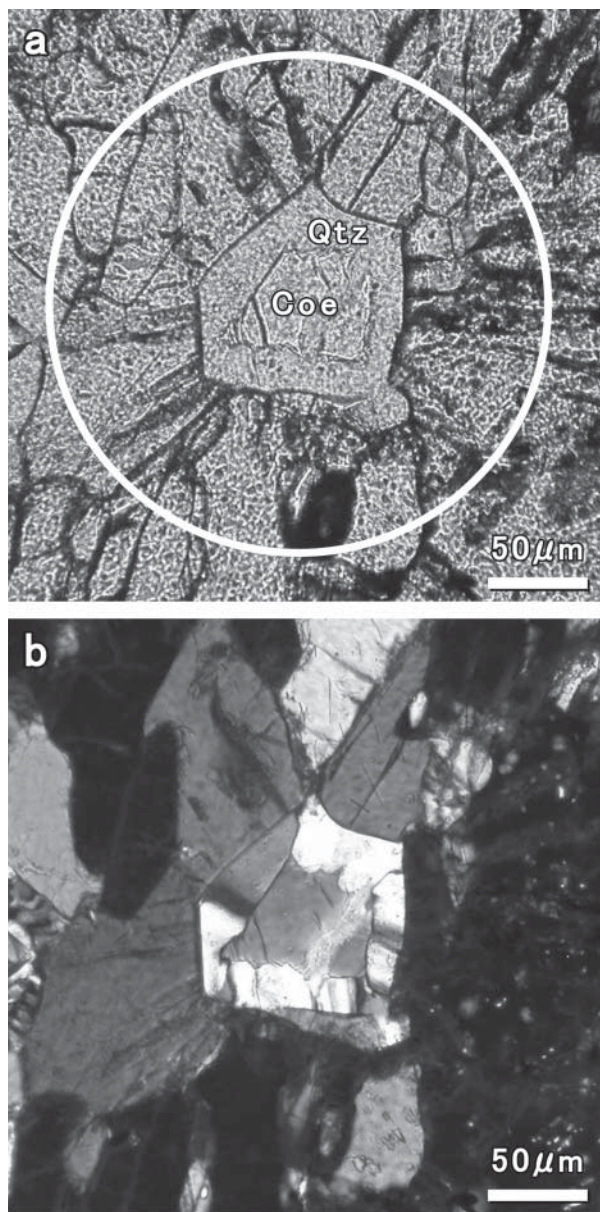

FIGURE 1. Coesite mantled by retrograde quartz crystals in the Sulu UHP rock. (**a**) Photomicrograph under plane-polarized light. A circle of 250 µm diameter shows the area irradiated by X-rays. (**b**) Photomicrograph under cross-polarized light.

located at the center of radial cracks. Coesite in the Sulu UHP rocks also occurs in this manner. We made a thin section of a Sulu rock sample and successfully found a coesite-like mineral in the section (Fig. 1a). The coesite occurs in quartz surrounded by grains of garnet and omphacite. Under cross-polarized light, it can be seen that the quartz surrounding coesite is composed of several tiny crystals (Fig. 1b).

The powder XRD pattern of the ground rock is shown in Figure 2, in which peaks of three main minerals, garnet, omphacite and phengite, are observed but quartz and coesite were not detected explicitly, suggesting low modal abundance.

X-ray diffraction study through the rock thin section

The rock thin section (~30 µm thick) on a typical slide glass ($2.8 \times 4.8 \times 0.135$ cm) was mounted on a Nonius Kappa-CCD four-circle diffractometer equipped with a collimator of diameter 250 µm. The size of the coesite crystal is about 60 µm and the aggregate size including a coesite and quartz crystals is about 100 µm, as shown in Figure 1. A device was designed for holding the glass thin section on the top of a goniometer head. The thin section was oriented such that the glass side faced the X-ray source and the sample side faced the detector. This arrangement enables the X-ray beam to pass through the glass first and then radiate the rock thin section. This is essential for clear diffraction spots without diffusion created by the slide glass. The diffraction pattern from the rock thin section is immersed in the background of amorphous diffraction from the relatively thick slide glass (0.135 cm thick). One of the data-collection frames is shown in Figure 3a as an example of the X-ray intensity distribution. The figure exhibits several diffraction spots from minerals of the rock thin section in the concentric intensity distribution of background that originated from the slide glass. The glass slide only, without the rock thin section, was also mounted on the diffractometer and the background intensity distribution was measured separately for each diffraction frame, which was subtracted from the original diffraction pattern for each frame. A frame of background intensity distribution, and a diffraction pattern from which the background was subtracted, are shown in Figures 3b and 3c, respectively. The diffraction spots are seen clearly in Figure 3c.

Intensity data collection and data reductions

There are three limitations to data collection. First, the incident X-ray beam should pass through the slide glass before it irradiates the rock thin section to minimize the effect of diffuse reflections. This setting limits the volume of reciprocal space that is accessible for data collection. Second, since a large glass slide instead of a small single crystal is mounted on the diffractometer, the four circles of the diffractometer are constrained to limited ranges of rotation to avoid collision between the glass slide and the body of the diffractometer. Third, under certain diffraction geometries that occur when the glass thin section makes a low angle with the incident beam, the slide glass shadows a part of the collection frame. One of the examples is shown in Figure 4.

Despite these limitations to data collection, a sufficient number of diffraction data from the rock thin section can still be collected. The data include diffraction spots not only from coesite or quartz but also from all the minerals within the circle of the diameter of collimator 250 µm (see Fig. 1a).
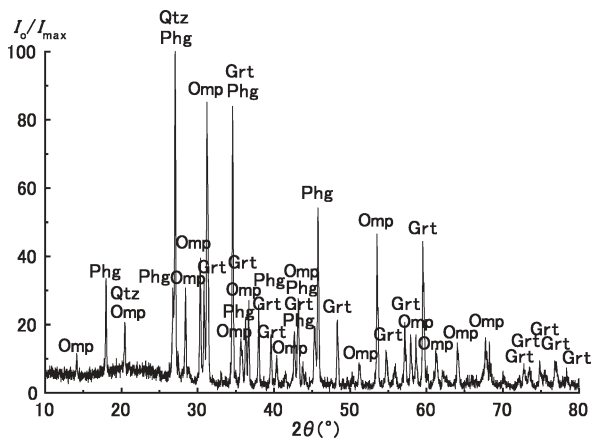

FIGURE 2. The powder XRD pattern of a ground specimen of Sulu UHP rock irradiated by Cu*K*α X-rays.
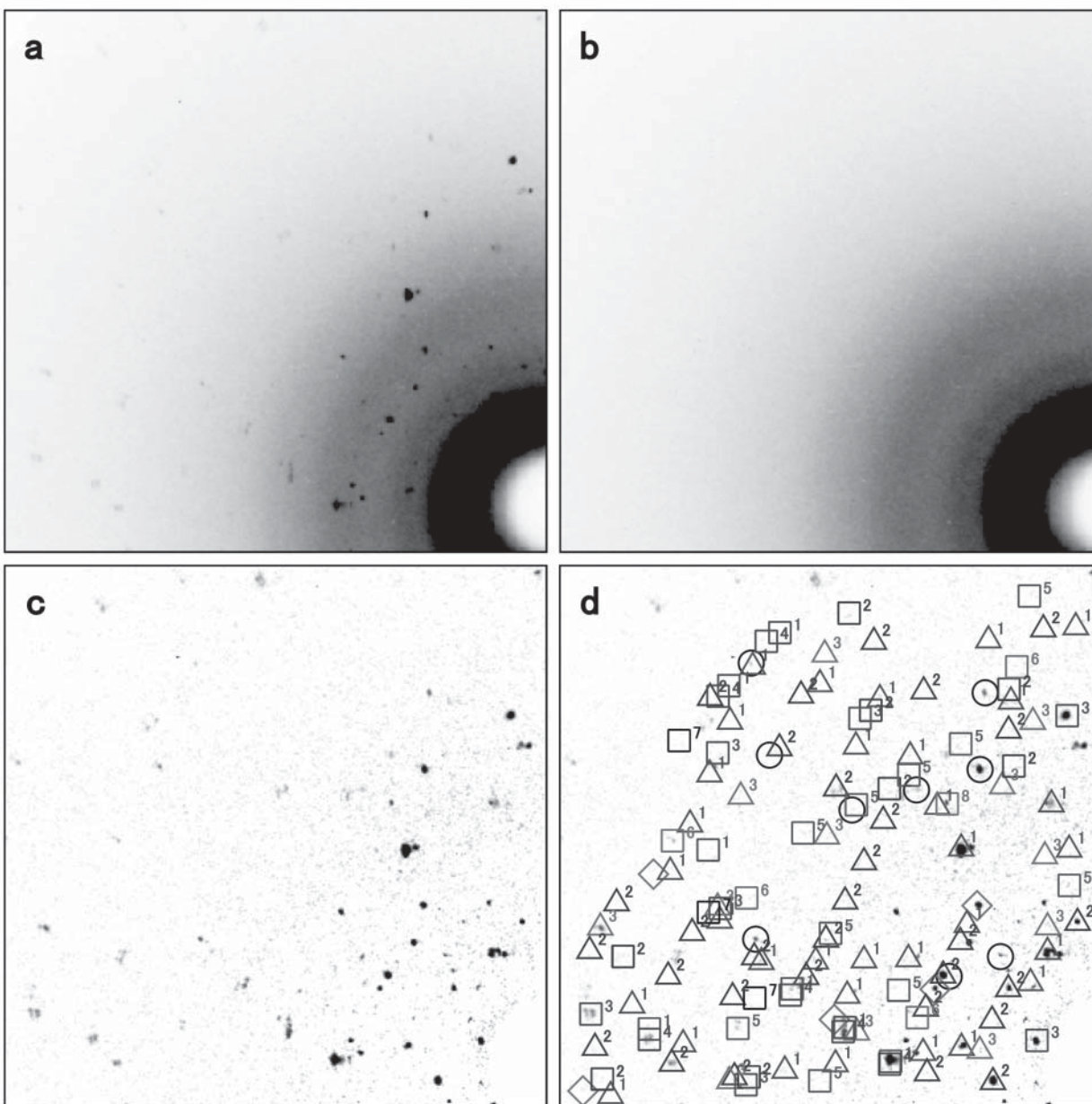
FIGURE 3. Four XRD pattern frames. (**a**) A CCD XRD pattern frame of the rock thin section on the slide glass. (**b**) A CCD XRD pattern frame of the slide glass without thin section. (**c**) The XRD pattern of the rock thin section from which the background of the slide glass is subtracted. (**d**) The XRD pattern in which the spot origins are assigned to each mineral. Open circle specifies a coesite; open diamond = a quartz; open triangles = three garnets; open squares = eight omphacites.

To extract the diffraction data of coesite or quartz from the multi-phase data, a suite of computer programs called ISSAC was written. The spots of a specific mineral in the thin section were identified using estimates of its cell parameters, space group, and intensities of reflections obtained from JCPDS cards or some other sources. The reciprocal lattice of the target mineral is constructed from the input data and this lattice is rotated to obtain coincidence of generated lattice points with observed diffraction spots, within a reasonable tolerance. Once a good coincidence is found for several diffraction spots, the orientation of the mineral can be obtained and all the spots that belong to the target mineral can be identified. All observed diffraction spots that coincide with generated lattice points are registered as spots reflected from the specific mineral. A flow diagram of the ISSAC code is shown in Figure 5.

The program correctly assigned the diffraction spots to the appropriate minerals and found two sets of data from a coesite and a quartz grain, and other sets from eight omphacites and three garnets (Fig. 3d). The orientation of each mineral was also determined. A few diffraction spots could not be identified, as is also shown in Figure 3d. In some cases, spots from different minerals were superimposed or otherwise were too close together to separate. These spots were discarded from further use. In total, 1760 intensity data from coesite and 320 intensity data from quartz were collected. Experiment conditions and crystal data are listed in Table 1. Experimental conditions for setting of the diffractometer are listed in the footnote of Table 1, in which scan speed = 0.167°/min, and $\Delta\varphi$ and $\Delta\omega$ = 1°/frame are included (for instance, exposure time was determined to be 6 min/frame). The incident X-ray beam first passes through the glass slide and the slide reduces the
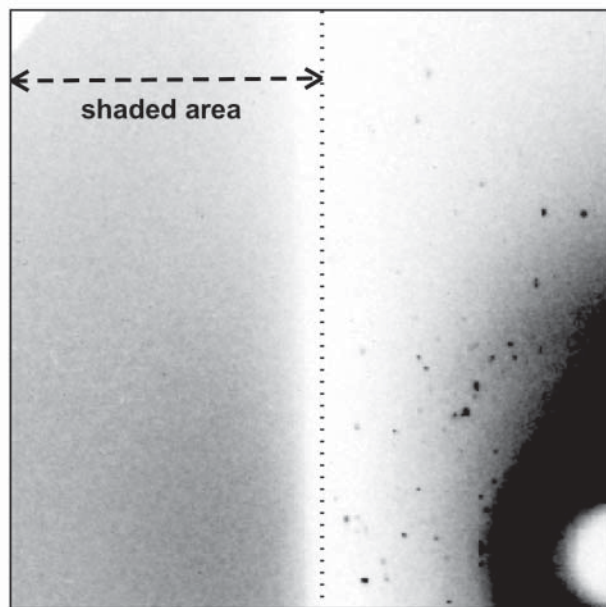
FIGURE 4. An example frame of a diffraction pattern recorded on a CCD in which the diffraction was intercepted by the slide glass. The shaded left half is the area intercepted by the slide glass.
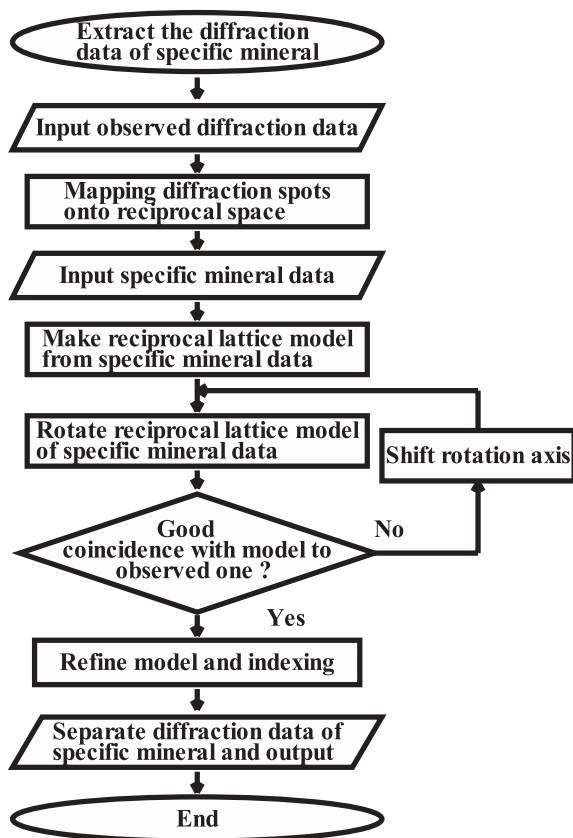

Relative path length through the slide glass fixed to unity for vertical irradiation
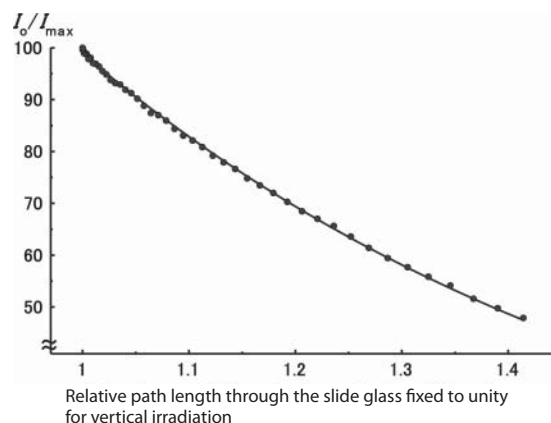
FIGURE 6. X-ray intensity reduced by the relative path length of the X-ray beam as it passes through the slide glass. The unity in the abscissa indicates the relative path length when the X-ray beam radiates vertical to the slide glass.

TABLE 1. Experimental conditions and crystal data of UHP coesite and quartz

		Coesite	Quartz
Space group		$C2/c$	$P3_221$
Unit-cell parameters	a (Å)	7.140(1)	4.923(1)
	b	12.371(1)	4.923(1)
	c	7.175(1)	5.409(1)
	α (°)	90	90
	β	120.34(1)	90
	γ	90	120
Unit-cell volume (Å³)		546.98(13)	113.53(4)
Z		16	3
Total measured reflections		1760	320
Observed unique reflections		593	153
R_{int}		0.065	0.150
$R(F)$		0.0459	0.0866
$R_w(F^2)$		0.0854	0.1897
Variable parameters		57	14

Note: Experimental conditions = Mo$K\alpha$ radiation, 30mA, 50kV, beam diameter = 250 μm; Scan set = Set. 1 (φ-scan) φ = –30~60°, ω = 180°, κ = 0°, θ = 0°, detector-to-sample distance = 25 mm; Set. 2 (φ-scan) φ = -60~25°, ω = 180°, κ = 0°, θ = 0°, detector-to-sample distance = 35 mm; Set. 3 (ω-scan) ω = 156~203°, φ = –23.98°, κ = 0°, θ = 0°, detector-to-sample distance = 25 mm; Set. 4 (ω-scan) ω = 200~209°, φ = –23.98°, κ = 69.39°, θ = 0°, detector-to-sample distance = 27.5 mm; Scan speed (all sets) = 0.167°/min; Δφ and Δω = 1°/frame; frame size = binned mode, 625 × 576 pixels.

FIGURE 5. ISSAC flow chart outlining the software algorithm used to identify the diffraction spots of a particular phase.

beam intensity before the beam irradiates the rock thin section, depending on the path length associated with the angle of the slide to the beam. The X-ray intensity reduction was measured as a function of the path length of the X-ray beam in the slide glass as shown in Figure 6, which yielded the linear absorption coefficient of the slide glass (μ = 11.45 cm⁻¹). The intensity data were corrected for the reduction of the incident beam. The rock thin section itself (~30 μm thick) is thin enough such that its absorption can be ignored since the X-ray path length through the thin section is always short. Nonetheless, the absorption correction was still made for incident and diffracted beams, assuming a plate-shaped specimen. In this correction, it was assumed that the incident and diffracted beams pass through the infinite plate-shaped specimen but the X-ray is diffracted only from the crystal with a size that is approximately defined by the crystal shape.

After these corrections and averaging of the symmetry related peaks, 593 and 153 unique reflections were obtained for structure analyses of coesite and quartz, respectively. These reflections successfully yielded the cell parameters of coesite and quartz that are listed in Table 1. This is the first confirmation by an X-ray study that the minerals are indeed coesite and quartz. The intensity data reductions and cell-parameter refinements were done with the DENZO and SCALEPACK suite of programs (Otwinowski and Minor 1997) and with the ISSAC suite of programs. All structure solutions and refinements were performed using the CRYSTALS suite of programs (Betteridge et al. 2003). The structures were refined to an *R*-factor of

TABLE 2. Structure data of UHP coesite and quartz

Atom	x		y		z		U_{11}		U_{12}		U_{13}		U_{22}		U_{23}		U_{33}		U_{iso}/U_{equiv}
Refined positional and thermal parameters for coesite
Si1	0.1401	(3)	0.1083	(2)	0.0723	(3)	0.015	(1)	−0.001	(1)	0.008	(1)	0.012	(1)	−0.001	(1)	0.015	(1)	0.014
Si2	0.5068	(3)	0.1581	(2)	0.5407	(3)	0.017	(1)	−0.001	(1)	0.009	(1)	0.013	(1)	0.000	(1)	0.015	(1)	0.015
O1	0.0000		0.0000		0.0000		0.016	(4)	−0.008	(3)	0.008	(3)	0.013	(3)	−0.006	(3)	0.017	(4)	0.016
O2	0.5000		0.1162	(5)	0.7500		0.020	(4)	0.000		0.010	(3)	0.015	(3)	0.000		0.012	(3)	0.015
O3	0.2669	(8)	0.1236	(4)	0.9406	(8)	0.022	(3)	−0.006	(2)	0.013	(2)	0.024	(3)	−0.005	(2)	0.018	(3)	0.020
O4	0.3104	(8)	0.1042	(4)	0.3275	(8)	0.023	(3)	−0.008	(2)	0.009	(2)	0.021	(3)	−0.005	(2)	0.016	(2)	0.020
O5	0.0167	(8)	0.2120	(4)	0.4780	(8)	0.021	(3)	−0.001	(2)	0.014	(2)	0.014	(3)	0.001	(2)	0.021	(2)	0.017
Refined positional and thermal parameters for quartz
Si	0.468	(2)	0.000		0.000		0.026	(7)	0.007	(4)	−0.004	(3)	0.014	(8)	−0.008	(7)	0.023	(6)	0.022
O	0.414	(5)	0.264	(4)	0.121	(3)	0.033	(16)	0.015	(12)	0.004	(10)	0.023	(9)	−0.008	(8)	0.030	(10)	0.028

0.046 and 0.087 for coesite and quartz, respectively, using anisotropic displacement factors for all the atoms. The final structure parameters are listed in Table 2.

Experimental validity of the new method

To examine the validity of using rock thin sections for crystal-structure determination, both the new and the conventional methods were applied to quartz in a granitic rock. A rock sample of the Oomine granite, collected at Tenkawa-mura, Nara, Southwest Japan, was used for the experiment. A quartz single crystal of 50 μm size was picked out of the rock sample and mounted on a Nonius Kappa-CCD four-circle diffractometer, and intensity data were collected in the conventional method. The data were corrected numerically for the absorption of the crystal shape. A rock thin section was also prepared from the same rock sample and one of the quartz crystals in the thin section was irradiated with X-rays to collect the intensity data. The crystal size of quartz in the rock thin section is about 120 μm (Fig. 7). The data collection and reduction for the thin section were accomplished in the same manner as for the Sulu rock sample. The procedures for the structure determination were performed in the same way both for the extracted crystal and the thin section. The R-factors for the extracted crystal and thin section samples converged to 0.020 and 0.029, respectively and the results are listed in Tables 3 and 4. Both of the techniques produced essentially the same results within the experimental errors, which assures the validity of the new thin section method.

DISCUSSION

In this study, a rock thin section on a slide glass was subjected to a direct XRD analysis, and the presence of coesite and retrograde quartz in a UHP rock was confirmed and crystal structure details were determined.

A single-crystal XRD technique that is applicable to thin sections containing a variety of minerals has been established for the first time in this study. Our method to identify and characterize minerals in a thin section on a slide glass has a wide range of applications. It can apply not only to other minerals in UHP rocks such as diamond and ringwoodite but also to minerals in any type of rocks, such as in a meteorite. Our method also separates the diffraction spots of a specific target mineral from other spots, as well as providing characteristic in situ information on the degree of crystalline perfection by analyzing the shapes of the spots (sharp, diffused, streaked, etc.). In our study, all the diffraction spots of coesite and quartz are sharp, indicating that the minerals are well-crystallized. Our method also yields the orientation matrix of each mineral in a thin section, which can be used to examine the in situ orientational relationships among the constituent phases. We determined the orientations of coesite, quartz, eight omphacites, and three garnets, but the meaning of the orientation relationships are not discussed in this paper. Our method is also applicable to a new or unknown mineral in a thin section. After the diffraction spots that originate from other known minerals are discarded, we can construct the lattice of the unknown mineral from the residual spots and determine its

TABLE 3. Experimental conditions and crystal data of granitic quartz

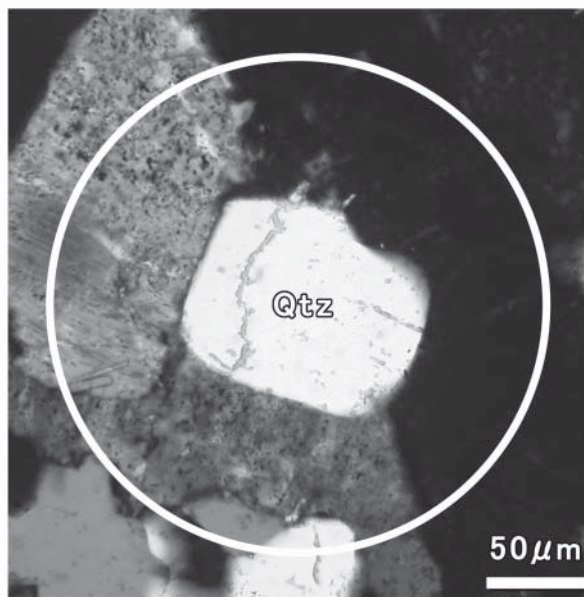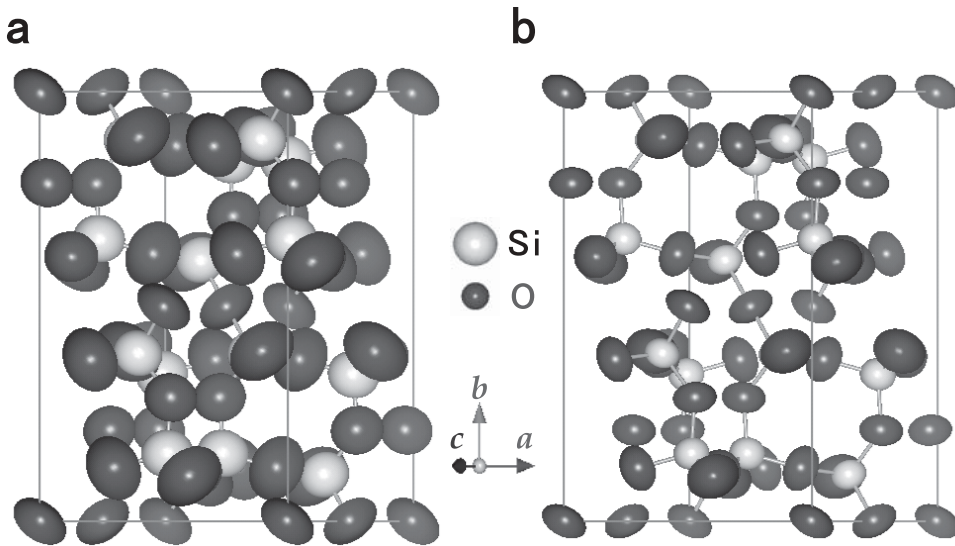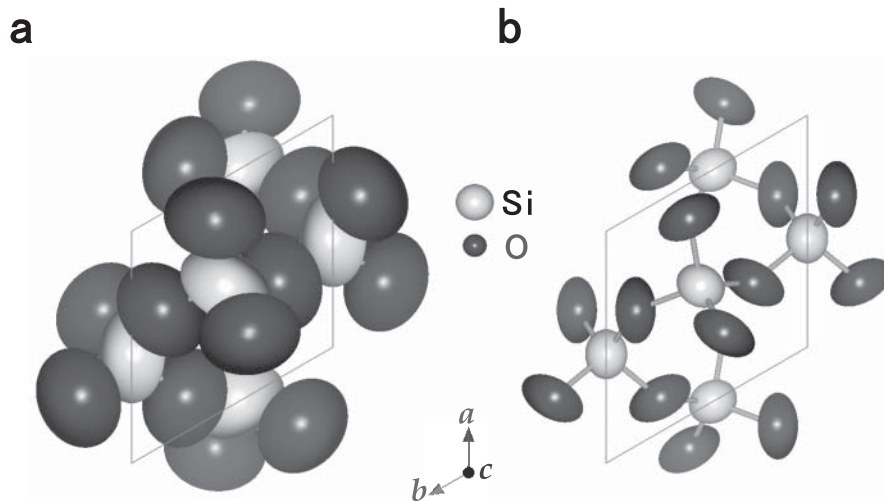|		Extracted crystal	Thin section
Space group		$P3_221$	$P3_221$
Unit-cell parameters	a (Å)	4.918(1)	4.917(5)
	c	5.407(1)	5.410(5)
Unit-cell volume (Å³)		113.26(4)	113.27(19)
Z		3	3
Total measured reflections		1145	396
Observed unique reflections		187	171
R_{int}		0.037	0.041
R(F)		0.0199	0.0288
$R_w(F^2)$		0.0417	0.0531
Variable parameters		14	14

FIGURE 7. Photomicrograph under cross-polarized light of quartz in the Oomine granite. The circle of diameter 250 μm shows the area irradiated by X-rays.

crystal structure. Our method provides a direct way to conduct XRD studies of minerals in a rock thin section.

The results of the structure determinations for coesite and quartz that are listed in Tables 1 and 2 are essentially consistent with previous studies at ambient conditions (Levien and Prewitt 1981; Angel et al. 2001, 2003; Levien et al. 1980; Kihara 1990). The R-factor for the quartz is fairly high and higher than that for the coesite. This difference arises from the fact that the target quartz comprises many tiny crystals transformed from the central coesite and smaller than coesite (Fig. 1), and intensities diffracted

TABLE 4. Structure data of granitic quartz

Atom	x	y	z	U_{11}	U_{12}	U_{13}	U_{22}	U_{23}	U_{33}	U_{iso}/U_{equiv}
Refined positional and thermal parameters for quartz										
Extracted crystal										
Si	0.4696 (2)	0.0000	0.0000	0.0090 (5)	0.0034 (3)	−0.0002 (2)	0.0069 (5)	−0.0003 (3)	0.0065 (5)	0.0077
O	0.4132 (5)	0.2679 (4)	0.1191 (3)	0.0166 (10)	0.0097 (8)	−0.0039 (8)	0.0123 (11)	−0.0036 (7)	0.0113 (10)	0.0123
Thin section										
Si	0.4702 (4)	0.0000	0.0000	0.0096 (7)	0.0043 (5)	−0.0001 (5)	0.0086 (11)	−0.0002 (10)	0.0099 (6)	0.0095
O	0.4137 (9)	0.2672 (7)	0.1194 (4)	0.0170 (20)	0.0098 (17)	−0.0019 (16)	0.0127 (14)	−0.0043 (12)	0.0144 (13)	0.0135

a   **b**

FIGURE 8. Crystal structures of coesite illustrated in the form of thermal ellipsoids at 99.99% probability. (**a**) Coesite determined by this study for Sulu UHP rocks. (**b**) Synthetic coesite reported by Angel et al. (2003) at 1 atm.

a   **b**

FIGURE 9. Crystal structures of quartz illustrated in the form of thermal ellipsoids at 99.99% probability. (**a**) Quartz determined by this study for Sulu UHP rocks. (**b**) Natural quartz reported by Kihara (1990) at room conditions.

from the quartz are very weak, which is inferred from the fairly high value of R_{int}, 0.150, compared with 0.065 for coesite. The crystal structures of Sulu coesite and its rim quartz are illustrated in the form of displacement ellipsoids and can be compared with those of synthetic coesite (Angel et al. 2003) and natural quartz (Kihara 1990) in Figures 8 and 9,[1] respectively. It is clear that the crystal structures of Sulu coesite and quartz agree with those reported previously, and the shapes of displacement ellipsoids,

although larger than those reported previously, are reasonable. The large displacement amplitudes can be ascribed to the extent of positional deviation from the average for each atom. The Sulu coesite is mantled by quartz, as shown in Figure 2, which demonstrates that the rim part of the former coesite has transformed to quartz, while the core remains as coesite (Nishiyama 1998). Large anisotropic displacement parameters provide evidence of trapped strain, frozen into the structure during the phase transformation from coesite to quartz, which is consistent with the record of adiabatic isothermal decompression path from the mantle (Yoshida et al. 2004).

To compare the thermal factors of coesite and quartz in the

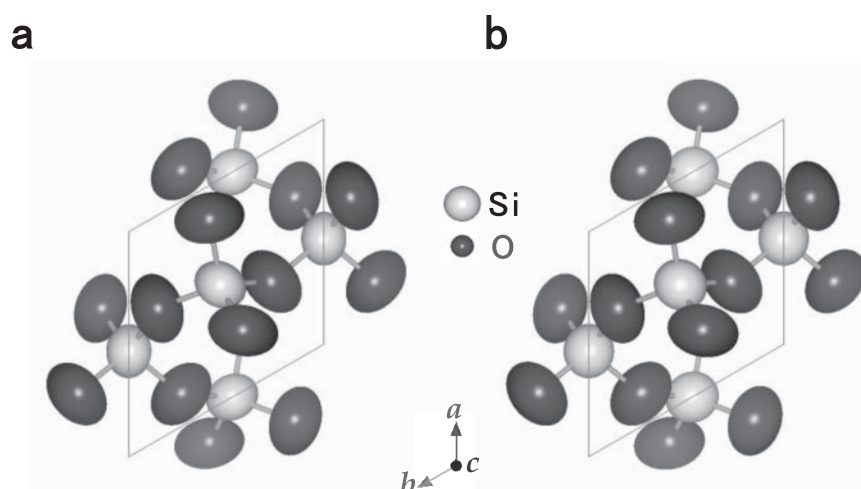[1] Figures 8, 9, and 10 were drawn using VENUS (Dilanian, R.A. and Izumi, F.) available at http://homepage.mac.com/fujioizumi/visualization/VENUS.html.

FIGURE 10. Crystal structures of quartz in the Oomine granite illustrated in the form of displacement ellipsoids at 99.99% probability. (**a**) Quartz determined by the conventional method using an extracted single crystal on a goniometer head. (**b**) Quartz determined by the new method using a rock thin section.

UHP rock and quartz in the granitic rock, the crystal structures for granitic quartz (using both the extracted crystal and the rock thin section) are illustrated in the form of displacement ellipsoids in Figure 10.[1] It is clear that there is no significant difference in the amplitudes of the displacement ellipsoids between the quartz structures determined from the extracted crystal and that in the thin section (Fig. 10), and that the difference in amplitudes between UHP quartz and natural one in Figure 9 is far larger than the difference of granitic quartz determined by the new method from thin section and the conventional method from an extracted single crystal. The displacement factors of UHP coesite were also derived by the same experimental procedures as in the case of UHP quartz, so it is reasonable to conclude that the large values found for the UHP coesite are similar in origin to those observed in the UHP quartz. From these results, we conclude that the large anisotropic displacement parameters of coesite and quartz in the Sulu rock are not an artifact from systematic problems encountered during the data-reduction stage through the new method, but represent actual features of the samples.

REFERENCES CITED

Angel, R.J., Mosenfelder, J.L., and Shaw, C.S.J. (2001) Anomalous compression and equation of state of coesite. Physics of the Earth and Planetary Interiors, 124, 71–79.

Angel, R.J., Shaw, C.S.J., and Gibbs, G.V. (2003) Compression mechanisms of coesite. Physics and Chemistry of Minerals, 30, 167–176.

Betteridge, P.W., Carruthers, J.R., Cooper, R.I., Prout, K., and Watkin, D.J. (2003) CRYSTALS version 12: software for guided crystal structure analysis. Journal of Applied Crystallography, 36, 1487.

Carswell, D.A. and Compagnoni, R. (2003) Introduction with review of the definition, distribution and geotectonic significance of ultrahigh pressure metamorphism. In D.A. Carswell, and R. Compagnoni, Eds., Ultrahigh Pressure Metamorphism, p. 3–9. Eötvös University Press, Budapest.

Chopin, C. (1984) Coesite and pure pyrope in high-grade blueshists of the Western Alps: a first record and some consequences. Contributions to Mineralogy and Petrology, 86, 107–118.

Hirajima, T. and Nakamura, D. (2003) The Dabie Shan-Sulu orogen. In D.A. Carswell, and R. Compagnoni, Eds., Ultrahigh Pressure Metamorphism, p. 105–144. Eötvös University Press, Budapest.

Hirajima, T., Ishiwatari, A., Cong, B., Zhang, R., Banno, S., and Nozaka, T. (1990) Coesite from Mengzhong eclogite at Dhonghai country, northeastern Jiangsu province, China. Mineralogical Magazine, 54, 579–583.

Hirajima, T., Wallis, S.R., and Zhai, M. (1993) Eclogitized metagranitoid from the Su-Lu ultra-high pressure (UHP) province, eastern China. Proceedings of the Japan Academy, 69, Series B, 249–254.

Ingrin, J. and Gillet, Ph. (1986) TEM investigation of the crystal microstructures in a quartz-coesite assemblage of the western Alps. Physics and Chemistry of Minerals, 13, 325–330.

Kihara, K. (1990) An X-ray study of the temperature dependence of the quartz structure. European Journal of Mineralogy, 2, 63–77.

Langenhorst, F. and Poirier, J.P. (2002) Transmission electron microscopy of coesite inclusions in the Dora Maira high-pressure metamorphic pyrope-quartzite. Earth and Planetary Science Letters, 203, 793–803.

Levien, L. and Prewitt, C.T. (1981) High-pressure crystal structure and compressibility of coesite. American Mineralogist, 66, 324–333.

Levien, L., Prewitt, C.T., and Weidner, D.J. (1980) Structure and elastic properties of quartz at pressure. American Mineralogist, 65, 920–930.

Nishiyama, T. (1998) Kinetic modeling of coesite-quartz transition in an elastic field and its implication for the exhumation of ultrahigh-pressure metamorphic rocks. The Island Arc, 7, 70–81.

Otwinowski, Z. and Minor, W. (1997) Processing of X-ray diffraction data collected in oscillation mode. Methods in Enzymology, 276, 307–326.

Smith, D.C. (1984) Coesite in clinopyroxene in the Caledonides and its implications for geodynamics. Nature, 310, 641–644.

Sobolev, N.V. and Shatsky, V.S. (1990) Diamond inclusions in garnets from metamorphic rocks: a new environment for diamond formation. Nature, 343, 742–746.

Tabata, H., Maruyama, S., and Shi, Z. (1998) Metamorphic zoning and thermal structure of the Dabie ultrahigh-pressure-high-pressure terrain, central China. The Island Arc, 7, 142–158.

Wallis, S.R., Ishiwatari, A., Hirajima, T., Ye, K., Guo, J., Nakamura, D., Kato, T., Zhai, M., Enami, M., Cong, B., and Banno, S. (1997) Occurrence and field relationships of ultrahigh-pressure metagranitoid and coesite eclogite in the Su-Lu terrain, eastern China. Journal of the Geological Society, London, 154, 45–54.

Yoshida, D., Hirajima, T., and Ishiwatari, A. (2004) Pressure-temperature path recorded in the Yangkou garnet peridotite, in Su-Lu ultrahigh-pressure metamorphic belt, eastern China. Journal of Petrology, 45, 1125–1145.